Nanotechnology, Science and Applications

Dovepress

open access to scientific and medical research

Open Access Full Text Article

ORIGINAL RESEARCH

Formulation and Characterization of Intranasal Drug Delivery of Frovatriptan-Loaded Binary Ethosomes Gel for Brain Targeting

Mohammed Layth Hamzah[1,2], Hanan Jalal Kassab[1]

[1]Department of Pharmaceutics, College of Pharmacy, University of Baghdad, Baghdad, Iraq; [2]Department of Pharmaceutics, College of Pharmacy, Uruk University, Baghdad, Iraq

Correspondence: Hanan Jalal Kassab; Mohammed Layth Hamzah, Department of Pharmaceutics, College of Pharmacy, University of Baghdad, Baghdad, Iraq, Email hanank@copharm.uobaghdad.edu.iq; mohammed.laith1100e@copharm.uobaghdad.edu.iq

Background: Frovatriptan succinate (FVT) is an effective medication used to treat migraines; however, available oral formulations suffer from low permeability; accordingly, several formulations of FVT were prepared.

Objective: Prepare, optimize, and evaluate FVT-BE formulation to develop enhanced intranasal binary nano-ethosome gel..

Methods: Binary ethosomes were prepared using different concentrations of phospholipid PLH90, ethanol, propylene glycol, and cholesterol by thin film hydration and characterized by particle size, zeta potential, and entrapment efficiency. Furthermore, in-vitro, in-vivo, ex-vivo, pharmacokinetics, and histopathological studies were done.

Results: Regarding FVT-loaded BE, formula (F9) demonstrated the best parameters from the other formulas; with the lowest particle size (154.1±4.38 nm), lowest PDI (0.213±0.05), highest zeta potential (-46.94±1.05), and highest entrapment efficiency (89.34 ±2.37%). Regarding gel formulation, G2 showed the best gel formula with drug content (99.82±0.02%) and spreadability (12.88 g/cm^2). In-vitro study results showed that, in the first 30 minutes, around 22.3% of the medication is released, whereas, after 24 hours, about 98.56% is released in G2.

Conclusion: Based on enhancing the bioavailability and sustaining the drug release, it can be concluded that the Frovatriptan-Loaded Binary ethosome Gel as nano-delivery was developed as a promising non-invasive drug delivery system for treating migraine.

Keywords: intranasal, frovatriptan, brain delivery, binary ethosome

Introduction

Migraines are among the most frequent headaches, affecting 17–18% of females and 6% of males. It is distinguished by attacks of acute unilateral headaches, nausea, and possibly a phobia of sounds or light.[1] The recurrent incidence of severe nausea, poor gastrointestinal (GI) absorption, or vomiting in migraineurs makes it more difficult to administer oral medications.[2–7] The intranasal approach is easy for the individual to use, painless, free from sterility restrictions, and non-invasive; it improves medication intake uniformity and speed while avoiding issues with self-injections and is created to address the shortcomings of the oral route.[8] Although several good migraine treatments have been created utilizing nasal delivery, most have not been proven commercially viable.[9–14] Some triptans can be administered nasally, demonstrating effective and fast action for relieving migraine attacks.[15] FVT has low penetration to the central nervous system (CNS).[16]

The terminal elimination half-life of FVT is around 26 hours, and it remains consistent regardless of age, gender, or renal function;[17] this suggests that frovatriptan may be especially suitable for people who experience protracted migraines and those who frequently experience migraines again. Nevertheless, FVT exhibits low oral bioavailability, ranging from 22% to 30%.[18] This long half-life, coupled with its poor oral bioavailability, makes it a potential target for nanotechnology delivery to improve its bioavailability. Since this direct main target is the brain, the intranasal route was chosen to represent the optimal delivery to the brain; additionally, this route will reduce its systemic side effects. FVT exhibits no impact on cytochrome P450 (CYP450)

Received: 14 November 2023
Accepted: 29 December 2023
Published: 16 January 2024

isoenzymes, making it improbable that it will influence the metabolism of other medications. Age, renal function, and mild to severe hepatic impairment do not require any dosage modifications.[17,19]

Ethosome is a special liposome manufactured utilizing a highly concentrated alcohol solution.[20] The binary ethosome (BE), which are improved ethosome, is made by mixing ethanol and propylene glycol in a particular ratio.[21] BE are more flexible, more effective at encapsulating drugs, have a larger drug loading capacity, and have better intrinsic dermal penetration-enhancing properties than liposomes.[15] BE in the nasal passages can be a local carrier for slowly released hydrophilic and lipophilic medications.[22]

While intranasal (IN) drug delivery is an attractive option,[23] the challenge for the formulator is great when attempting to find a method to infiltrate the mucus lining of the nasal canal without inflicting irreversible tissue damage. The main disadvantages are small nasal cavity capacity (0.2 mL), anterior leakage, and mucociliary clearance, which might impair the effectiveness of the nasal medication delivery system.[24–28] In situ, gels provide several advantages over typical gels, such as being simpler to produce, injectable as a liquid, and able to remain on the nasal cavity's surface for a longer time owing to gelling and mucoadhesion.[29,30] The current study aims to prepare, optimize, and evaluate FVT-BE formulation to develop enhanced intranasal binary nano-ethosomes.

Materials and Methods

Materials

Frovatriptan succinate (CAS Number: 158930-17-7) was purchased from Pharmaffiliates (Catalogue number: PA 06 83000, India), Poloxamer 407 was purchased from Sigma-Aldrich® Solutions, Germany (CAS Number: 9003-11-6, ID: 16758), Carbopol 934 was purchased from HiMedia Laboratories LLC, USA (stock keeping unit: GRM6761), (Hydroxypropyl)methyl cellulose K100 was purchased from Otto Chemie Pvt. Ltd., India (CAS: 9004-65-3, HSN Code: 39123919, and Code: H 1815), and Dialysis Membrane-135 was purchased from HiMedia Laboratories LLC, USA (stock keeping unit: LA398), phospholipon ® 90H [Phospholipids, hydrogenated, with 70% phosphatidylcholine] was purchased from Pharma Excipients ™ (CAS-No. 97281-48-6), the remaining chemicals and reagents were of analytical grade and procured from local vendors.

Formulation and Characterization of BE Formulations

Formulation of BE

Binary ethosomes were formulated using the standard mechanical dispersion thin-film hydration approach with a rotating flash evaporator (IKA® - Werke GmbH & Co.KG, Germany). PL 90H, cholesterol, propylene glycol (PG), and the drug were dissolved in ethanol (10–40 mL), placed in the rotary evaporator flask, and allowed to rotate at 60 rpm for 20 minutes; this allowed the drug-lipid layer to settle in the flask's interior after ethanol evaporation, and the flask was left overnight in a desiccator to evaporate any lingering ethanol. Hydro ethanol solutions of varying concentrations were used to rehydrate the drug-lipid film by spinning it at 100 rpm for 30 minutes at a temperature higher than the lipids' glass transition temperature. Then, probe sonication (SH 70G, Bandelin Sonopuls UW 2070, Berlin, Germany) was used for roughly 25 minutes at a frequency of 5 minutes each cycle 3 sec interval time, and ten cycles to transform the vesicles into unilamellar vesicles. The finished ethosome formulation was kept cold in the fridge; the formulas are illustrated in Table 1.

Characterization of FVT-Loaded BE Dispersion

Measurement of vesicle size and polydispersity and zeta potential BE's particle size and zeta potential were determined using Zetasizer Malvern Ultra Red, Worcestershire, UK). Polydispersity index and zeta size of BE were measured at 25±1°C by diluting 50 µL of the vesicle dispersions with 50 µL of deionized DW in folded capillary cell DTS 1070 before taking any readings; each sample had three independent estimates. Zeta potential (ZP) was measured in a reusable universal dip cell kit.[31]

Determination of Entrapment Efficiency (EE%)

The ultracentrifugation technique was used to determine the EE% of BE formulations. Samples were centrifuged (Sigma 3–30KHS, Sigma Laborzentrifugen GmbH, Germany) for 3 hours at four °C and 25000 revolutions per minute (rpm).

Table 1 Formulation and Characterization of BE Formulations

Formula	PL (w/v)	Ethanol (mL)	PG (w/v)	Ch (mg)	PBS (Up to mL)
	1	0	0	0	45
2	3	0	0	0	45
3	1	20	5	1	45
4	2	20	7.5	1	45
5	3	20	10	1	45
6	4	20	15	1	45
7	1	10	5	1	45
8	1	20	7.5	1	45
9	1	30	10	1	45
10	1	40	15	1	45
11	2	10	5	0.5	45
12	2	20	7.5	1.5	45
13	2	30	10	1.5	45
14	2	40	15	2	45
15	4	10	5	1	45
16	4	20	7.5	1	45
17	4	30	10	1	45
18	4	40	15	1	45
19	3	10	5	1	45
20	3	20	7.5	1	45
21	3	30	10	1.5	45
22	3	40	15	1	45
23	1	10	10	1	45
24	2	20	10	1	45
25	3	30	10	1	45

Abbreviations: PL, Phospholipon® 90H [PL90H], PBS, Phosphate-buffered saline, Ch, cholesterol, PG, Propylene glycol.

The supernatant was used to calculate EE% was calculated using the following Equation, and the FVT concentrations in the supernatant were measured by UV spectrophotometer (Perkin-Elmer, λ35, Waltham, MA, USA) at 255 nm.[32,33]

$$EE(\%) = \frac{W_{intialdrug} - W_{freedrug}}{W_{intialdrug}} x10$$

Effect of Different Variables on FVT BE

Effect of Different Amounts of Phosphatidylcholine

F1, F3, F7, F8, F9, F10, and F23 (containing 0–40% ethanol) were created with 1% w/v concentrations of PL90H, PG (0–15%); in addition, F2, F5, F19, F20, F21, F22, and F25 (containing 0–40% ethanol) were created with 3%, w/v concentrations of PL90H, and PG (0–15%). F4, F11, F13, F14, and F24 (containing 10–40% ethanol) were created with 2% w/v concentrations of PL90H

and PG (5–15%); while F6, F15, F16, F17, and F18 (containing 10–40% ethanol) were created with 4%, w/v concentrations of PL90H, and PG (5–15%), were used to see the effect of formula variables on particle size and EE%.[34]

Effect of Different Amounts of Cholesterol

To illustrate the effect of cholesterol on particle size and EE%, the formulas F2, F11, F9, F21, and F14 were created using 0, 0.5, 1, 1.5, and 2 mg of cholesterol.[35]

Incorporation of Optimized Formulation (F9) into Intra-Nasal Gel Formulations

Preparation of Intra-Nasal Gel Formulations from F9

Poloxamer 407 was dispersed in 80 mL of cold Distilled water and allowed complete hydration overnight. Then, Carbopol or HPMC powder was added gradually to the poloxamer dispersion. At the same time, on a magnetic stirrer (Intelli-Stirrer MSH-300i, Biosan, USA), the FVT BE dispersion was added to this dispersion, and the volume was completed with distilled water,[36–38] as illustrated by Table 2.

Characterization of FVT BE Gel

pH and Visual Appearance

The pH must be considered one of the most crucial elements to formulate FVT effectively. The gel used nasally should have a pH close to that of the nose so as not to irritate. The pH of the BE gel was determined using a digital pH meter.[34] Visual examination was used to assess the homogeneity, the presence or absence of any aggregation in its physical appearance.[31]

Measurement of Spreadability by Parallel-Plate Technique

The precise quantity of FVT BE gel required on a clear glass slide was weighed (300 µL). Another slide was placed on top of the gel-coated one. Loading gel included placing a 100 g weight on the top slide, which caused the gel to spread evenly throughout the slides and leave no traces on the sides. Pulley was secured to the top slide with a constant weight attached.[39–42] The time it took for the top slide to travel the distance between the two slides was recorded, starting at zero seconds. Spreadability is found in the following Equation:

$$S = \frac{M \times L}{T}$$

Spreadability (S), Mass (M), Length (L), and Time (T) are all variables that determine how far a glass slide can be slid in a given amount of time.

Determination of Gelation Temperature

The visual inspection method was used to determine the gelation temperature of the prepared FVT BE gel.[43–45]

Table 2 Formulation of FVT BE-Loaded Gel from the Optimized Formula (F9)

Formulation	F9 dispersion (mL) (2.5 mg/mL)	Poloxamer 407 (g)	Carbopol 934 (g)	HPMC K100 (g)	DW (mL)
G1	10	14	0.5	–	100
G2	10	14	1.0	–	100
G3	10	14	1.5	–	100
G4	10	14	–	0.5	100
G5	10	14	–	1.0	100
G6	10	14	–	1.5	100
G7	10	14	1.0	1.0	100

Abbreviations: DW, distilled water; HPMC, (Hydroxypropyl) methylcellulose.

Thermostatically controlled digital magnetic stirring at a rate of 10°C /min was used to raise the temperature of a beaker that contained 10 mL of FVT BE. The beaker was tilted to visualize gelation, and the temperature at which the beaker was tilted at 90 degrees and did not flow due to the gel formation was recorded as the gelation temperature.

Drug Content

The drug content of formulations was evaluated in triplicate with a double-beam UV visible spectrophotometer (Shimadzu UV-1800). One milliliter of the formulation was placed in a 10-milliliter volumetric flask, and the remaining 9 milliliters were double-distilled water. A 1 mL sample was prepared by diluting the original solution with 10 mL of double-distilled water. As a last step, a UV-visible spectrophotometer[46] was used to determine the absorbance of the solution after it was created.

Evaluation of FVT BE F9 and G2 Gel

Differential Scanning Calorimetry

BE was optimized via thermal analysis of FVT powder, poloxamer 407, PL, FVT BE dispersion F9 (lyophilized), and FVT BE optimized gel (spread and allowed to dry) using a 4000 model from VEGA, Tescan, EasyProb, and Czech Reb. Aluminum pans were used to dry the samples (10 mg each) using dry nitrogen as the flowing gas. These thermograms were obtained between 20–300 °C, with the temperature rising at 20 °C per minute.[47]

Fourier Transform Infrared Analysis

To examine the drug, phospholipid, physical mixture, and optimal loaded BE formulations, FT-IR spectrometer 8300, Lambda Scientific, Australia; we opted for the diamond horizontal attenuated total reflectance (ATR) sample attachment (PerkinElmer, France). A 4-cm resolution was used to scan the samples between 4000 and 6000 cm.$^{-1}$[48]

Morphology by Scanning Electron Microscopy (SEM)

Utilizing scanning electron microscopy (SEM), the morphology of FVT BE was examined (SEM, Hitachi, Tokyo, Japan) by diluting a drop of BE formulation was diluted in double-distilled water (DW) (1 in 100) and then air-dried on a sample holder. A range of magnifications and accelerating voltages, up to 15,000 volts, were then used to examine the sample under vacuum.[49]

In vitro Release Study

The release study was conducted on the FVT solution (2.5 mg), the optimized BE (F9), and the selected BE gel prepared from F9 (G2). The researchers studied the diffusion of drugs in different formulations using a Franz diffusion cell.[50] A diffusion membrane with a molecular weight cut-off range of 12,000–14,000 kDa was employed for dialysis. The dialysis membrane was immersed in a phosphate buffer solution with a pH of 6.4 for 24 hours before the commencement of the test. The diffusion cell was filled with 21 mL of phosphate buffer solution at a pH of 6.8, and a dialysis membrane was affixed to the cell. The gel, which contained a medication corresponding to a dosage of 2.5 mg, was applied to the donor chamber. A circulating water bath regulated the 32–34°C temperature. Samples of 1 mL were extracted at various time intervals (0.5, 1, 3, 6, 12, and 24 hours) and subsequently substituted with an equal volume of the new solution. These samples were then filtered, and the quantity of the drug present was measured using a UV-visible spectrophotometer set at a wavelength of 255 NM.

Ex-Vivo Drug Permeation Study

The animal handling was done in accordance with both the Office International des Epizootics (OIE) principles on animal ethics guidelines and AVMA guidelines.[51] The euthanasia procedure involved the intravenous administration of pentobarbital sodium (100 mg/kg) to three healthy lambs at the age of 6 months. Following the demise of the subjects, the lambs underwent decapitation. Subsequently, the distinct components of the nasal cavity, namely the nasal concha and septum, were submerged in a solution consisting of PBS medium supplemented with 5% double antibody and 1% amphotericin and gentamicin. Subsequently, the distinct variations of the nasal cavity were carefully placed into a 50 mL centrifuge tube pre-filled with phosphate-buffered saline (PBS) and antibiotics. Following the agitation of the container, it was subjected to a series of washing procedures, repeated 3 to 4 times. Each wash cycle was conducted for a duration of 5 to 10 minutes. After the completion of the process, the washed nasal tissue was carefully transferred onto a sterile plate. The nasal mucosa tissue was carefully removed using ophthalmic scissors and tweezers.

Furthermore, a segment of the nasal mucosa is extracted and carefully positioned on a fresh, clean plate, ensuring that the surface is upward. Subsequently, the nasal mucosa is processed, transforming it into consistently shaped circular tissue blocks with a diameter of 8 mm, employing a tissue sampler. The nasal cavity is multifaceted, featuring diverse mucosal thicknesses and epithelial features across several regions. The current research has concentrated on the mucosa located on the inferior nasal concha within the respiratory region of the nasal cavity. On average, around 40 specimens of mucosal tissue can be procured from the nasal cavity of sheep that are six months old. The mucosal tissue underwent pretreatment and was subsequently positioned on a 12-hole transwell apparatus, with the mucosal surface oriented upward. The membrane of the top chamber filter had a pore diameter measuring 0.4 μM. Approximately 600 μL of culture media was introduced into the complete transwell device, with a thickness of only half that of the mucosal tissue. The tissue was cultured at 37°C and in an atmosphere containing 5% carbon dioxide. The culture medium was refreshed regularly.[52,53]

The ex-vivo study was conducted on the FVT solution (2.5 mg), the optimized BE (F9), and the selected BE gel prepared from F9 (G2). At 34 degrees Celsius, 12 milliliters of phosphate buffer saline (pH 6.8) were added to the acceptor chamber and agitated with a magnetic stirrer. After incubating the donor part for 30 minutes, selected formulations (FVT solution, F9, and G2) were added. One mL aliquots of samples were taken out at regular intervals up to 24 hours and replaced with phosphate buffer saline pH 6.8. As the dust settled, a spectrophotometer set to 255 nm was used to examine the samples. The drug formulations' permeability coefficients (in cm/s) were determined with the use of the following formula,

$$\text{Permeability coefficient} = \left(\frac{d_c}{d_c}\right)_{ss} x \frac{V}{AC_d}$$

Where, $(dc/dt)_{ss}$ (μg mL^{-1} s^{-1}) change of concentration under steady-state; A (cm^2) is the permeation area; V (mL) the volume of the receiver compartment; and C_d (μg mL^{-1} is the initial donor concentration.[54]

Histopathological Evaluation of Mucosal Tissue

After being treated in PBS (pH 6.8) or a diffusion chamber with the gel formulation, tissue samples were histopathologically examined. A 10% buffered formalin solution (pH 6.8) was used to fix the tissue. After being broken into smaller pieces and put on glass slides, paraffin blocks were stained with hematoxylin and eosin. A pathologist unaware of the Study's objectives examined tissue slices under a light microscope for ex vivo and drug permeation studies.[55]

In vivo Brain Targeting Study

FVT pharmacokinetic and brain distribution studies were established for intranasally delivered FVT BE gel G2 and FVT intravenous solution. The study includes a total of 78 Female rats (Wister albino rats), weighing 180–220 g, aged 2–3 months; these rats were randomly divided into three groups: group A (6 rats considered a negative control, which will be sacrificed early to obtain plasma and brain tissue to calibrate the HPLC to measure the drug concentration), group B (includes 36 rats, divided into six groups each contain six rats at each time of administration of the drugs, after 30 minutes, after 1 hour, after 3 hours, after 6 hours, after 12 hours, and after 24 hours) given FVT IV solution at dose 0.257 mg/kg, and group C (includes 36 rats, divided into six groups each containing six rats at each time of administration of the drugs, after 30 minutes, after 1 hour, after 3 hours, after 6 hours, after 12 hours, and after 24 hours) given FVT binary ethosome in situ gel intranasally (IN) at dose 0.257 mg/kg, as illustrated in Figure 1. Following completion of therapy, all animals were anesthetized intraperitoneally (I.P.) with 80 mg/kg of ketamine and 10 mg/kg of xylazine. Following total anesthesia, all rats were sacrificed by carbon dioxide.[51,56] After the end of each group's experimental period, dissection was done for the euthanized rat, and the plasma and brain tissue were removed and weighed for further analysis.

The rats were obtained from the (Animal Facility of the College of Pharmacy – Baghdad University, Baghdad, Iraq), housed in polypropylene cages under a temperature-controlled environment (25 °C), with an inverted light-dark cycle (12/12 hours), and acclimated for ten days before starting the experiment at the same center where the rats were obtained (Animal Facility of the college of pharmacy – Baghdad University, Baghdad, Iraq). The animals were maintained on a standard pellet diet and free access to water ad libitum supplied by the Animal Facility of the College of Pharmacy – Baghdad University.

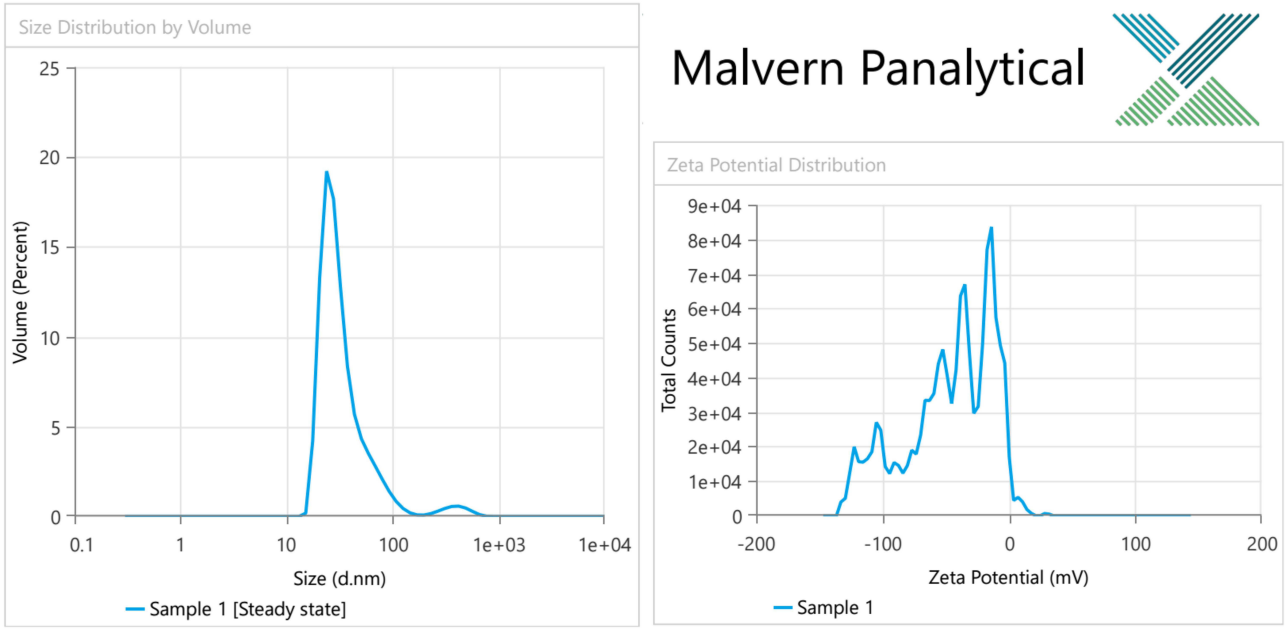

Figure 1 Particle size and zeta potential of optimal TVF loaded BE (F9).

Dosing

The usual human dose of FVT is 2.5 mg (per 60 kg) per day; based on the Reagan-Shaw study,[57] this dose is converted to animal dose (rat) based on the following equation:[57]

$$\mathrm{HED}\left(\frac{\mathrm{mg}}{\mathrm{kg}}\right) = \mathrm{AED}\left(\frac{\mathrm{mg}}{\mathrm{kg}}\right) \mathrm{x} \frac{\text{Animal } K_m}{\text{Human } K_m}$$

HED is the human dose, AED is the animal dose, and K_m is the conversion factor (for human adults, it is 37, and for rats, it is 6).[57] Based on this equation, the animal dose was 0.257 mg/kg.

Sample Preparation for Analysis

Plasma Treatment

Utilizing a cooling centrifuge (Z216MK, Hermle Labortechnik GmbH, Germany). The blood sample was centrifuged for 10 minutes at 4000 rpm to separate the plasma, then stored at 80 °C. For the sake of analysis, 500 µL of each of the plasma samples was combined with 100 µL of the "internal standard DILT solution" (1000 ng/mL) and 1 mL of "acetonitrile". The mixture was vortexed for 30 seconds (Vortex, IKA MS3 Digital, Germany) and then centrifuged for 15 minutes at 6000 rpm. HPLC was used to determine the amount of FVT in the supernatant.[58]

Brain Treatment

Each piece of the obtained tissue from the rat brain was homogenized (Heidolph Diax 900, Germany) for one minute at 25,000 rpm with three times the volume of ordinary saline. Brain homogenates underwent the same processing steps as plasma samples to determine their FTV content.[59]

HPLC Analysis of FVT-Succinate

The HPLC system (Agilent Technologies 1200 series, Germany) consisting of a G1315D diode array detector, an LC-G 1311A solvent delivery pump with a 20-µL loop, and a rheodyne sample injector was employed. The mobile phase, which was composed of "acetonitrile and potassium phosphate buffer" (10 mM) 35:65 (v/v), was adjusted to pH 5.5 with orthophosphoric acid and ran on an Agilent® TC-C18 column (250 mm 4.6 mm I.D, particle size 5 m) at 30 °C. The injection volume was 50 L, and the elute was seen at 255 nm with a 1 mL/min flow rate.[60]

Pharmacokinetic Analysis

Using the WinNonlin® application, the determination of pharmacokinetic parameters Cmax, Tmax, $AUC_{0\text{-}360}$, $t_{1/2}$, and mean residence time (MRT) in both plasma and brain was done for each treatment (was calculated as the ratio between the area under the first moment curve and the corresponding $AUC_{0\text{-}360min}$) (Version 2, Pharsight Co., Mountain View, CA, USA). Following intravenous injection, the absolute (F_a) and relative (F_r) bioavailabilities of FVT were estimated using the following equations:[61]

$$F_a = \frac{AUC^{0}_{360\ min}(IN)}{AUC^{0}_{360\ min}(IV)} X100$$

$$F_r = \frac{AUC^{0}_{360\ min}(IN)\ x\ Dose_{IV}}{AUC^{0}_{360\ min}(IV)\ x\ Dose_{IN}} X100$$

To evaluate brain targeting efficiency, two indices, namely drug targeting efficiency (DTE%) and brain drug direct transport percentage (DTP%), were calculated using the following equations:[61]

$$DTE\% = \frac{\left(\frac{AUC_{brain}}{AUC_{blood}}\right)IN}{\left(\frac{AUC_{brain}}{AUC_{blood}}\right)IV} X100$$

$$DTP\% = \frac{(B_{IN} - B_X)}{B_X} X100$$

$$BX = \frac{(B_{IV})}{(P_{IV})} X100$$

Where "Bx" represents the brain "AUC" fraction contributed by systemic circulation through the blood-brain barrier following (IN) administration, B_{IV} is the $AUC_{0–360}$ (brain) following IV administration, P_{IV} is the $AUC_{0–360}$ (blood) following IV administration, B_{IN} is the $AUC_{0–360}$ (brain) following IN administration, P_{IN} is the $AUC_{0–360}$ (blood) following IN administration.[45,62]

Ethical Consideration

The University of Baghdad approved the study – College of Pharmacy, Research Ethical Committee (approval name: RECAUBCP532022G, approval date: 5-2-2022).

Sample Size and Randomization

For sample size computation, program G Power was utilized[63] based on Cohen's principles.[64] A table of random integers was used to construct the groupings at random; the animals were placed in labeled containers and given tail tags to minimize misunderstanding.[65]

Statistical Analysis

The current study used GraphPad Prism version 10.0.1 for the statistical analysis. The descriptive statistics were reported as mean ± standard deviation (S.D.). The independent *t*-test was applied to verify the significance of the difference between the studied groups, followed by the post hoc Tukey's test. The differences between the groups were considered significant statistically when the P-value was ≤0.05.

Results and Discussion

Characterization of FVT BE

Effect of Different Amounts of Phosphatidylcholine, Cholesterol, and Ethanol

As seen in Table 3, regarding EE, the highest value was seen on F9, which was statistically significant compared to the other formulas, see Figure 2. Regarding PS, two formulas (F9 and F15) showed statistically the lowest PS compared to other formulas,

Table 3 Characterization of FVT Loaded BE

Formulation	EE%	PS	PDI	ZP
F1	63.98±2.18[a]	352.69±5.37[a]	0.413±0.01[a]	−24.39±0.21[a]
F2	69.31±0.98[a]	494.83±2.64[b]	0.521±0.06[a]	−22.59±1.05[a]
F3	80.51±0.98[b]	200.37±2.64[c]	0.294±0.06[a]	−32.13±2.16[b]
F4	69.82±3.06[a]	265.49±2.84[d]	0.367±0.03[a]	−38.37±0.36[c]
F5	59.38±2.14[a]	326.49±9.62[e]	0.473±0.04[a]	−20.46±0.49[a]
F6	72.34±2.61[c]	264.72±7.34[d]	0.196±0.02[b]	−43.94±0.12[d]
F7	54.29±0.94[d]	268.31±9.31[d]	0.375±0.01[a]	−28.49±2.04[b]
F8	69.42±1.52[ac]	220.59±6.52[f]	0.322±0.06[ab]	−31.27±2.31[b]
F9	89.34±2.37[e]	154.1±4.38[g]	0.213±0.05[b]	−46.94±1.05[d]
F10	75.96±3.16[bc]	210.34±1.98[cf]	0.487±0.03[a]	−26.59±0.05[a]
F11	78.35±2.38[bc]	254.95±2.35[d]	0.203±0.05[b]	−38.37±0.07[c]
F12	62.54±0.97[a]	235.67±10.59[f]	0.386±0.04[a]	−26.04±0.04[a]
F13	49.37±0.35[d]	433.92±2.46[h]	0.495±0.01[a]	−29.38±0.05[b]
F14	45.12±3.59[f]	376.22±8.37[i]	0.512±0.03[a]	−39.07±0.28[c]
F15	74.39±1.05[bc]	147.35±1.39[g]	0.418±0.05[a]	−22.7 ± 2.3[a]
F16	70.34±2.13[ac]	234.51±8.31[f]	0.229±0.01[b]	−44.27±2.03[d]
F17	65.39±3.05[ac]	295.37±7.26[j]	0.324±0.03[a]	−33.15±1.06[b]
F18	64.51±2.03[a]	235.67±6.29[f]	0.367±0.05[a]	−36.41±1.34[c]
F19	69.42±1.52[ac]	220.59±6.52[f]	0.322±0.06[ab]	−31.27±2.31[b]
F20	60.53±2.37[ad]	394.28±4.38[i]	0.413±0.05[a]	−32.13±2.16[b]
F21	55.96±3.16[d]	210.34±1.98[f]	0.487±0.03[a]	−26.59±0.05[a]
F22	68.35±2.38[ac]	254.95±2.35[cd]	0.361±0.05[a]	−28.37±0.07[b]
F23	62.54±0.97[a]	235.67±10.59[f]	0.386±0.04[a]	−26.04±0.04[a]
F24	49.37±0.35[df]	433.92±2.46[h]	0.495±0.01[a]	−29.38±0.05[b]
F25	75.12±3.59[bc]	295.22±8.37[j]	0.268±0.03[b]	−39.07±0.28[c]
p-value	<0.0001	<0.001	<0.001	<0.001

Notes: A column with different letters indicates significant differences (≤0.05) [[a] vs [b, c, d, e, f, g, h, i, j] ≤0.05; [b] vs [c, d, e, f, g, h, i, j]≤0.05; [c] vs [d, e, f, g, h, i, j]≤0.05; [d] vs [e, f, g, h, i, j]≤0.05; [e] vs [f, g, h, i, j]≤0.05; [f] vs [g, h, i, j]≤0.05; [g] vs [h, i, j]≤0.05; [h] vs [i, j]≤0.05; [i] vs [j]≤0.05].
Abbreviations: EE, entrapment efficiency; PS, particle size; PDI, polydispersity index; ZP, zeta potential.

see Figure 3. Regarding PDI, F6, F9, F11, F16, and F25 showed statistically lower PDI values than other formulas, see Figure 4. Regarding ZP, F6, F9, and F16 showed statistically highest negative charge compared to other formulas, as illustrated in Figure 5. Based on these findings, it is obvious that F9 had the best parameters out of the other formulas, see Figure 1.

Entrapment Efficacy (EE)

Because there is more lipid phase accessible to integrate the lipophilic FVT, the EE% changed from 80.51 ± 0.98 to 59.38 ±2.14% with an increase in PL 90H concentration from 1 to 4% w/v in F3, F4, and F5, respectively.[33] The entrapment somewhat decreased (72.34±2.61%) when the PL90H concentration was raised to 4% in F6; this could result from the

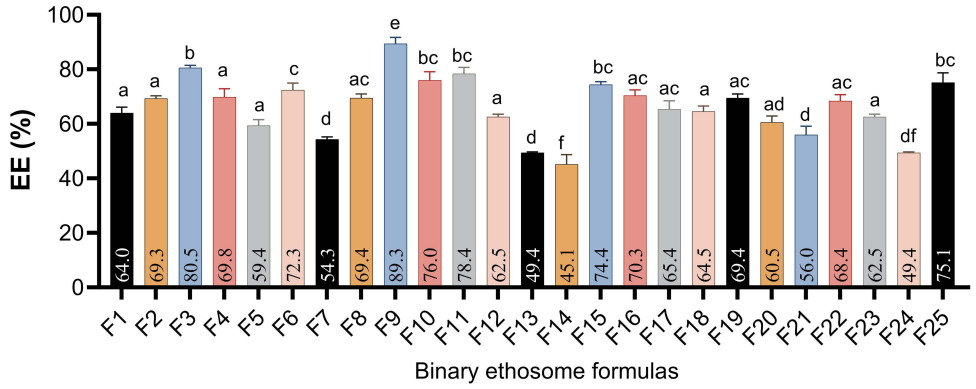

Figure 2 Entrapment efficiency (%) of various BE formulas [a column with different letters (a, b, c, d, e, and f) indicates significant differences (≤0.05)].

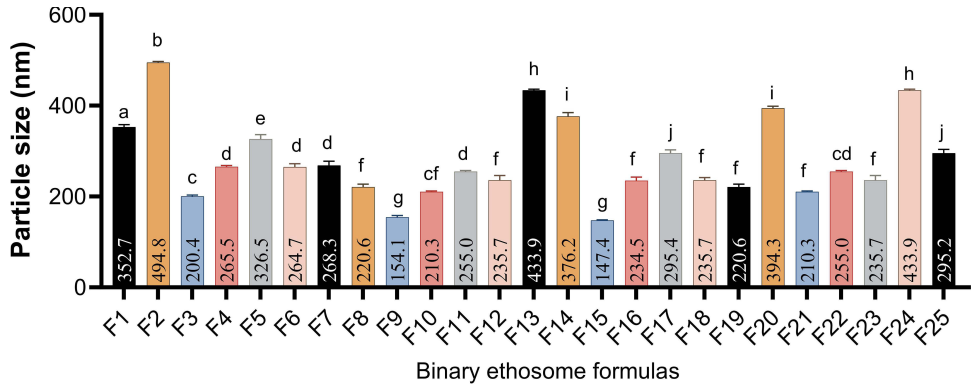

Figure 3 Particle size (nm) of various BE formulas [a column with different letters (a, b, c, d, e, f, g, h, i, and j) indicates significant differences (≤0.05)].

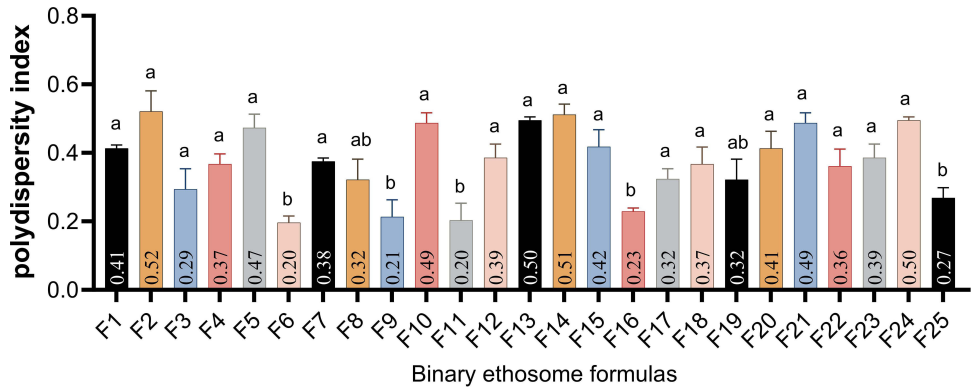

Figure 4 Polydispersity index of various BE formulas [a column with different letters (a, and b) indicates significant differences (≤0.05)].

likelihood of vesicle aggregation.[36] When the PL90H concentration was held constant at 1% w/v, an increase in the percentage of ethanol from 10% in F7 to 20% in F3 resulted in a significant increase in the EE%, with values of (54.29 ± 0.94% versus 80.51 ± 0.98%), when the ethanol percentage was further increased to 30mL (F9) or 40mL (F10), the EE percent increased significantly, with values of 89.34±2.37% and 75.96±3.16%, as demonstrated in Table 1 and Table 3. Formulas containing 2% PL, F4, F11 to F14, with an increase in ethanol concentration (from 10 to 40 mL), the EE% showed a significant reduction in value with higher ethanol contractions. More FVT can be trapped because ethanol, a co-solvent, makes FVT more soluble in the hydroalcoholic core and the vesicle membrane. It makes the bilayer

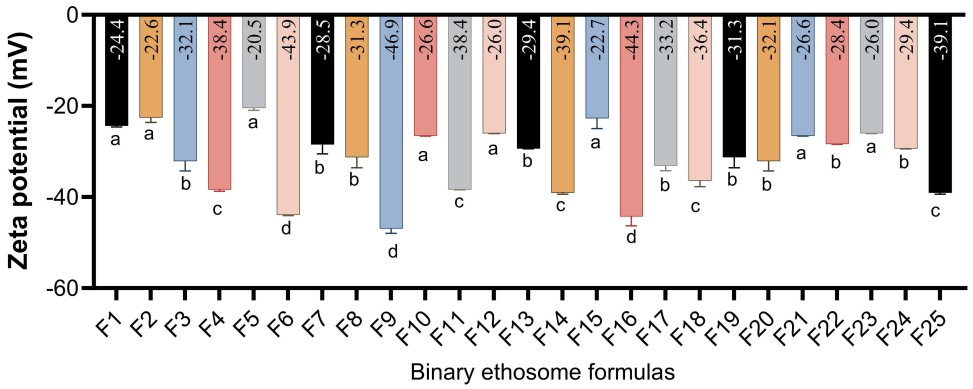

Figure 5 Zeta potential of various BE formulas [a column with different letters (a, b, c, and d) indicates significant differences (≤0.05)].

membrane more fluid, which improves FVT encapsulation. The vesicle membrane became more porous when the ethanol concentration was raised to 30% or 40%; however, the EE percent fell due to drug leakage.[66] EE is a crucial characteristic for gauging the intra-nasal drug delivery system and, by extension, its distribution potential. Because of its lipophilic nature, FVT is encased in a non-polar lipid bilayer. The aggregation and leaking of BE and the size of the vesicles themselves are strongly impacted by the formulation's physical stability, which in turn is affected by the ethanol and phospholipid contents. Vesicles leaked at high ethanol and propylene glycol concentrations, lowering the % EE and preventing the encapsulated drug from penetrating the intra-nasal layers.[40]

Particle Size (PS)

PS ranged from 147.35±1.39 nm to 494.83±2.64 nm. As the concentration of PL90H increases and ethanol concentration remains constant (F3 to F6, 20 mL ethanol, and F9, F13, and F17, 30 mL ethanol), PS size increases with higher PL90H in the formula. At 1% PL90H, as ethanol volume increases (10 to 30 mL), PS decreases (F7, F8, and F9). These results strongly suggest that phospholipids and ethanol do not interact with one another.

Also, the development of a hydrocarbon phase with interpenetrating capabilities suggests that ethanol and propylene glycol may have a disproportionate impact on vesicle size. Intra-nasal drug administration is greatly aided by smaller vesicles (300 nm) that can quickly pass through the mucus barriers and reach deep layers. FVT BE formulations with a vesicle size of 200 nm have been reported to be capable of intra-nasal penetration. FVT-loaded BE that have been prepared may pass through many mucus layers since their size is less than 200 nm.[67]

Nanoparticles, colloidal systems, and surfactants have been used to improve the brain absorption of active compounds such as tacrine, insulin, and human growth hormones. Vesicular carriers such as liposomes and niosomes based on amphiphilic compounds have also been investigated for nasal delivery to the brain. Recently, the approach of using modified phospholipid vesicles has received significant attention.[68]

Polydispersity Index (PDI) and Zeta Potential (ZP)

The generated dispersions had PDI values between 0.196 and 0.521 and ZP between −20.46±0.49 to -46.94±1.05 mV. At 1% PL90H and ethanol volume between 10 to 30 mL, PDI was reduced (higher PL90H shows the opposite effect), while at 40 mL ethanol, PDI started to increase. Fixing ethanol volume and increasing PL90H concentrations associated with increased PS. Similar findings were reported with ZP, in which increasing ethanol while fixing PL90H at 1% was associated with higher ZP, with lower PL90H associated with higher ZP. High negative zeta potential values were also linked to cationic solvents such as propylene glycol and ethanol. The chosen dispersion exhibited physicochemical properties well-suited to lipid BE used in the preparations.[69,70]

Evaluation of FVT-Loaded BE Gel

The pH and Visual Characteristics

The reported pH value of the investigated formula was (5.3 ± 0.03) within the acceptable range of the successful nasal formulation (between 5.3 and 7.0[71]). All the prepared BE dispersion formulas (G1 - G7) appeared as a homogenous creamy suspension without precipitation or aggregation with a characteristic ethanol odor, as illustrated by Table 4.

Gelation Temperature

The influence of mucoadhesive agents on formulation gelation temperature (Table 4) reflects the change in gelation temperature that is directly proportional to the mucoadhesive agent concentration.

Spreadability

The best spreadability for the FVT-loaded BE gel formula was seen in G2, with a 12.88 g/cm^2 spreading, as seen in Table 4.

Drug Content

A total drug concentration ranging from 92.54±0.13% to 99.82±0.02% was found in the tested FVT-loaded BE formulations; the best formula was G2, as seen in Table 4.

Evaluation of the Optimized FVT BE Formula

DSC Studies

The DSC thermogram of the FVT pure drug, FVT-loaded (F9), FVT-loaded BE gel (G2), and all the excipients (P407 and PL90H) necessary to make them are shown in the DSC thermogram. The FVT pure drug showed an endothermic peak at 182.41°C, indicating that FVT is pure and crystalline, associated with its melting point and breakdown. The optimized formula (F9) showed an endothermic peak of the drug at 102.75°C. The FVT-loaded in BE gel (G2) showed an endothermic peak of the drug at 104.92 °C. P407 peak at 55.52 °C. This reduction in the endotherm of the drug could be due to the mixing of drug and excipients, which lowered the purity of each component in the mixture and may not necessarily indicate potential incompatibility,[72] as illustrated by Figure 6.

FTIR Spectral Studies

The FTIR spectra of the drug in different polymer mixes were compared to the FTIR spectrum of the pure drug. FVT spectra showed a clear peak at 3120.94 and 3497.06 cm^{-1}, confirming the presence of the primary amide group in monohydrate form. Spectral bands at 827 and 1100 cm^{-1} indicate the presence of an aromatic group, whereas the peak at 1666.48 cm^{-1} is characteristic of the presence of a C=O bond. The drug is compatible with the gelling agent's poloxamer 407 and Carbopol 934, as shown by FTIR spectroscopy investigations of drug-polymer interactions, revealing weak physical contact. Figure 7

Table 4 Physical Evaluation of FVT BE Gel Formulations

	P407 (w/v%)	C934 (w/v%)	HPMC	Visual Appearance	pH	Gelation Temperature °C	Spreadability (g.cm/sec)	Drug Content (%)
G1	14	0.5	–	Milky appearance	5.8±0.01^a	33.9±0.21^a	9.68±1.31^a	92.57±0.21^a
G2	14	1.0	–	Milky appearance	5.3±0.03^b	33.7±0.43^a	12.84±2.43^b	99.82±0.02^b
G3	14	1.5	–	Milky appearance	5.1±0.01^b	31.9±0.13^a	6.57±1.27^a	95.43±0.14^c
G4	14	–	0.5	Milky appearance	5.4±0.02^b	34.2±0.26^a	7.64±0.98^a	98.54±0.37^d
G5	14	–	1.0	Milky appearance	6.0±0.01^c	30.09±1.00^a	6.82±1.34^a	94.21±0.28^e
G6	14	–	1.5	Milky appearance	6.2±0.02^d	28.9±2.30^b	5.37±1.29^c	96.56±0.11^f
G7	14	1.0	1.0	Milky appearance	6.5±0.01^e	35.6±3.21^a	7.81±1.17^a	92.54±0.13^a
p-value	-	-	-	-	<0.001	0.001	<0.001	<0.001

Notes: P407: Poloxamer 407 (w/v%), C934: Carbopol 934 (w/v%), HPMC: hydroxypropyl methylcellulose. A column with different letters indicates significant differences (≤0.05) [$^{a\ vs\ b, c, d, e, f}$≤0.05; $^{b\ vs\ c, d, e, f}$ ≤0.05; $^{c\ vs\ d, e, f}$ ≤0.05; $^{d\ vs\ e, f}$ ≤0.05; $^{e\ vs\ f}$≤0.05.].

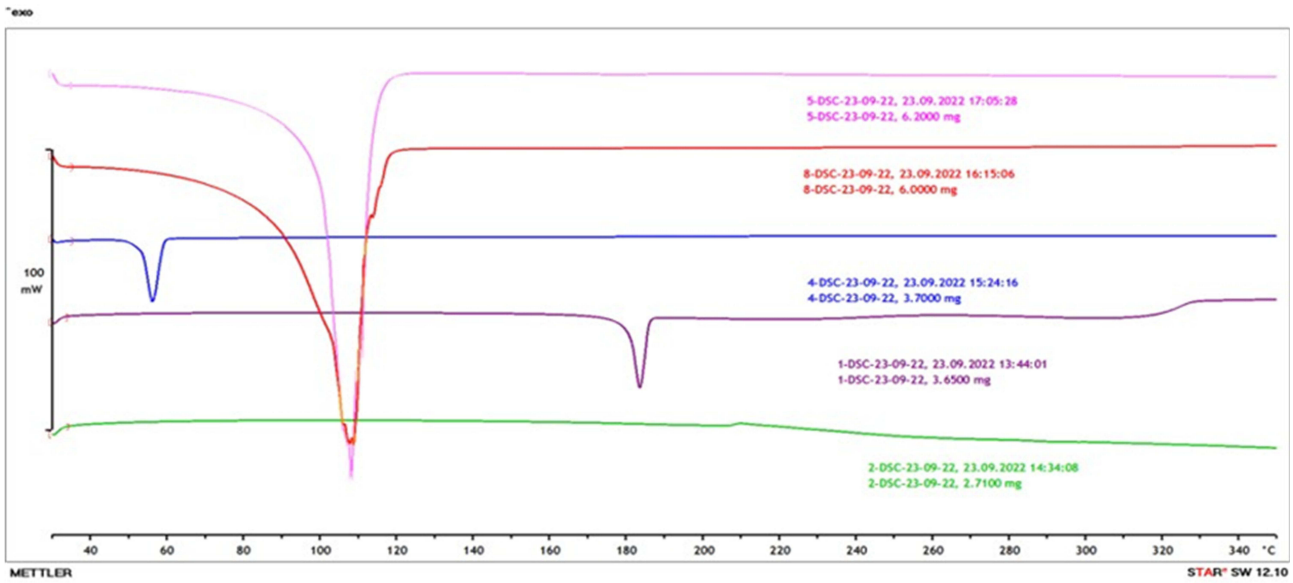

Figure 6 DSC Thermograms of 1) Pure Drug (FVT) [1-DSC], 2) Lipid (PL90H) [2-DSC], 3) Poloxamer 407 [4-DSC], 4) FVT-loaded BE (F9) [5-DSC], 5) FVT-loaded BE gel (G2) [8-DSC].

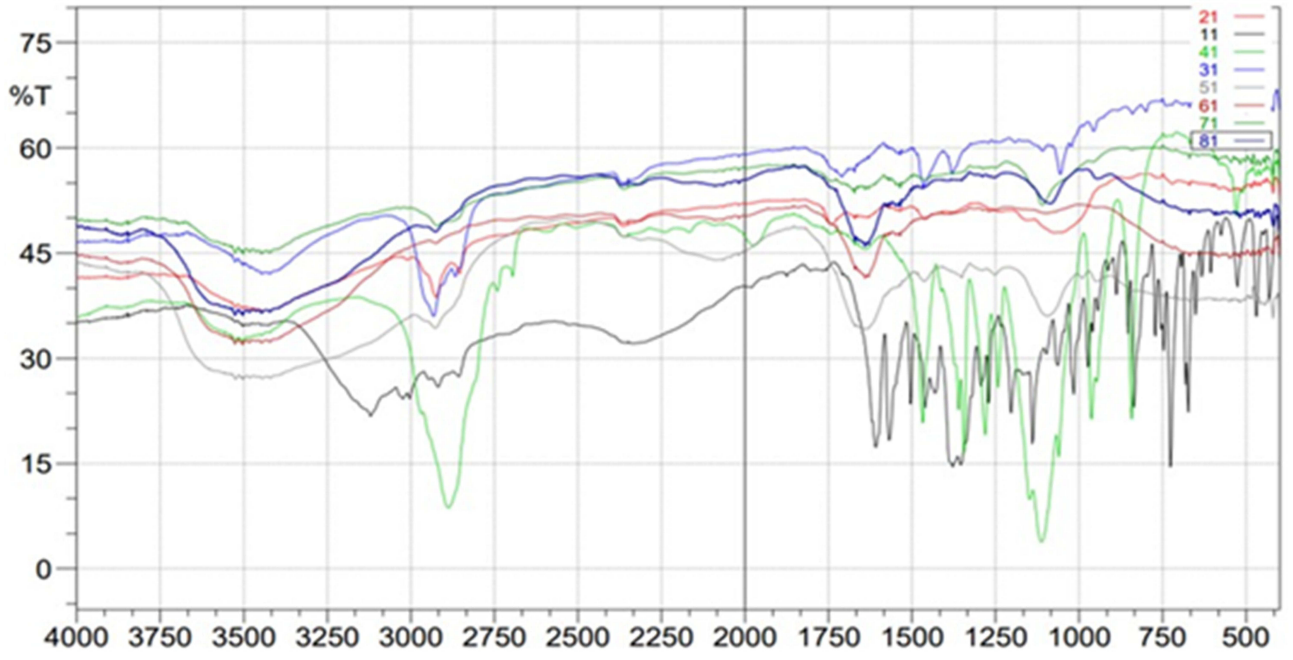

Figure 7 FTIR spectral studies of 1) Pure Drug (black line; line-11), 2) phospholipon 90H (red line; line-21), 3) Ethanol (white, blue; line-31), 4) propylene glycol (light green; line-41), 5) Poloxamer 407 (white gray; line-51), 6) F9 (dark red; line-61), 7) Carbopol 934 (dark green; line-71), 8) G2 (dark blue; line 81).

shows the FTIR spectra of the medication and a physical combination of FVT with poloxamer 407 and Carbopol 934. The peaks at 1690, 1810, 2530, 2900, and 3300 cm^{-1} were all present, but the strength of the peak at 3500 cm^{-1} was reduced, demonstrating the weak physical interaction.

Scanning Electron Microscopy

The spherical shape, homogenous particle size, excellent segregation, and monodispersed of the particles in the BE formulation and the enhanced BE gel both contribute to their remarkable stability (Figure 8). Particle size detected by SEM corresponds well with the Delsa Nano C analyzer. The presence of monodispersed particles demonstrated the

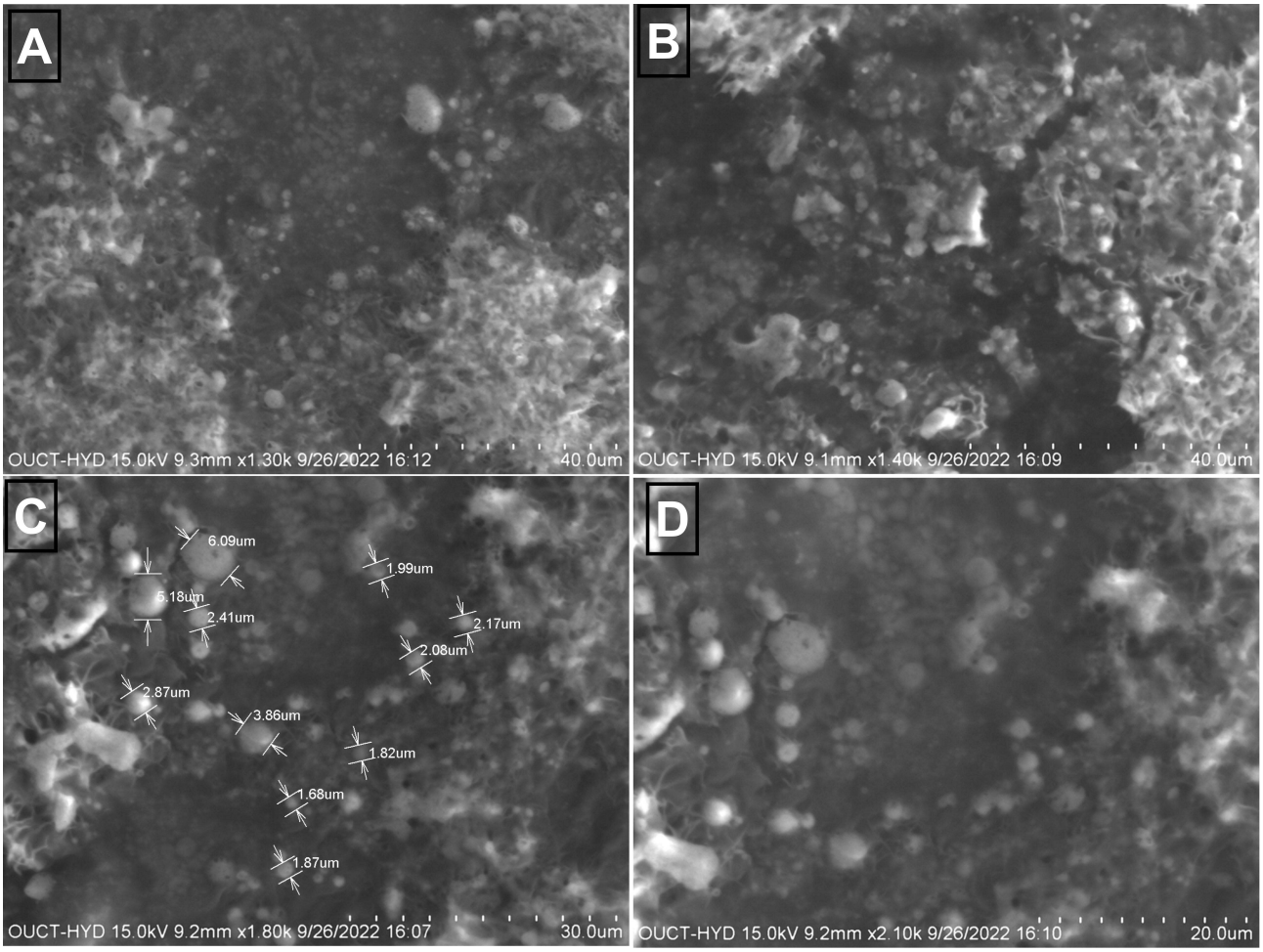

Figure 8 SEM images of optimized FVT-loaded BE F9 (**A** and **B**), optimized FVT-loaded BE gel G2 (**C** and **D**).

presence of sufficient surface charge on the outside of BE to maintain their separation. Additionally, the value of the zeta potential was negative, lending credence to the theory.

In-Vitro Cumulative Release Study

By analyzing how quickly the drugs were released from G2 and F9, we may deduce that the Carbopol's chemical composition is critical for facilitating drug release. A quick initial release was followed by a delayed maintenance release of the FVT-loaded in situ gel in G2. In the first 30 minutes, around 22.3% of the medication is released, whereas after 24 hours, about 98.56% is released (Figure 9).

Ex vivo Permeation Study

Ex vivo studies on lamb's nasal mucosa examined the drug penetration characteristics of FVT-loaded BE (G2). After 24 hours, those exposed to the G2 absorbed 496.38±2.21 mg/cm^2, but those exposed to the FVT solution absorbed just 148.32±1.64 mg/cm^2. The steady-state flow rate of the G2 was 6.985 mg/cm^2/h, whereas that of the FVT solution was only 1.896 0.14 mg/cm^2/h. When FVT was encapsulated in situ gel, the medication's permeability increased by around 3.68-fold compared to the drug solution, indicating that the therapy would diffuse through the nasal mucosa (Figure 10).

Histopathological Studies

Following seven days of exposure to FVT-loaded BE gel formulation, the anterior cross sections of the rat nasal canal in Figure 11 are shown in the light microscope. The mucosa and underlying cartilage can be shown in the micrographs to

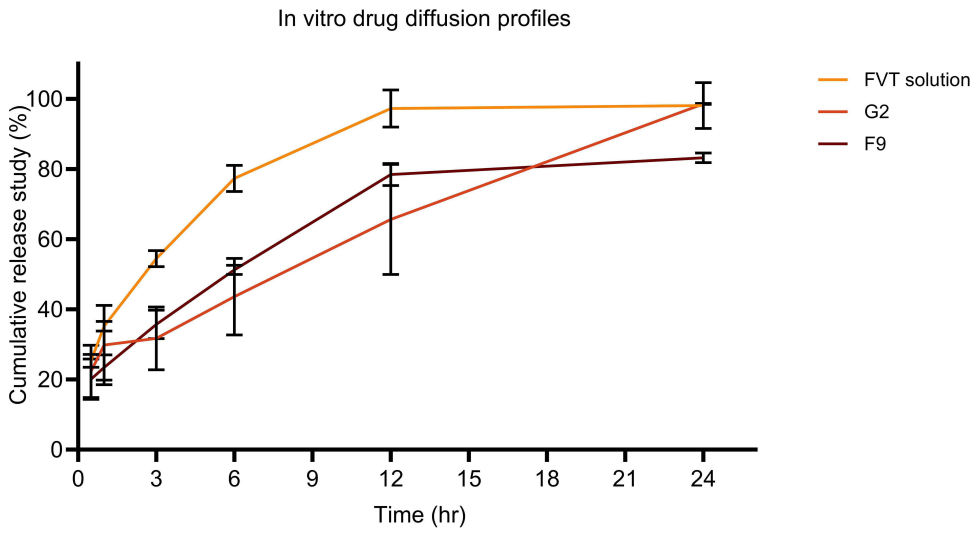

Figure 9 In vitro drug diffusion profiles of FVT solution, G2, and F9 formulation.

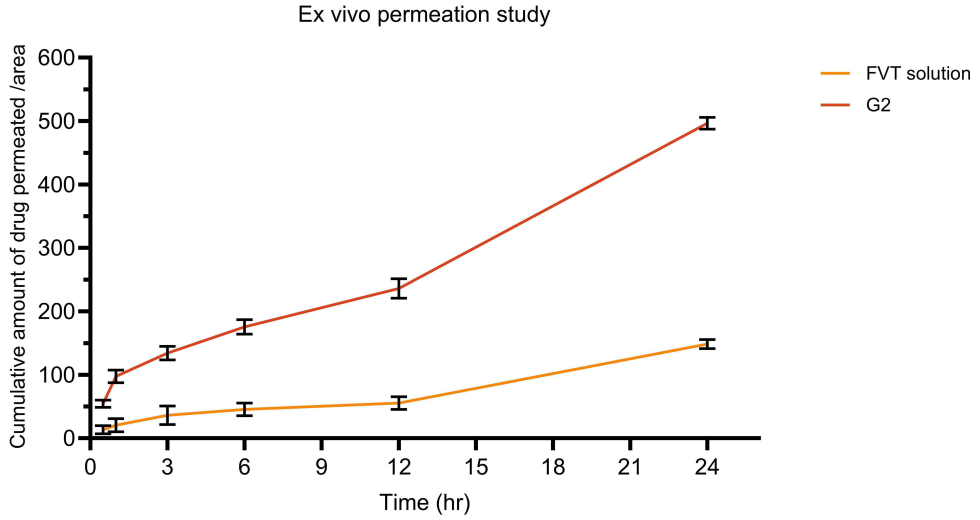

Figure 10 Ex vivo permeation study at nasal pH 6.4.

have a normal histological structure. The rats showed no severe necrosis, epithelial cell sloughing, or bleeding symptoms. However, just a slight edema in the mucosal layer's lamina propria was seen in the rats treated with FVT-loaded BE gel (G2) dispersion, and the rats treated with F9 likewise showed only a slight congestion of blood vessels in the lamina propria. These findings supported other literature,[73] and these formulations were selected for further clinical studies.

In vivo Study

FVT concentrations in rat plasma and brain were determined using a straightforward, well-validated modified HPLC technique.[60] With a total run duration of less than 15 minutes, it was discovered that the retention periods for FVT were 3.798 and 3.964 minutes for plasma and brain and 5.64 and 6.21 minutes for the internal standard. Peaks from the commercial formula and FVT were separated and resolved with acceptable symmetry. Individual blank serum was examined at FVT and marketed formulation retention durations, and no endogenous interference peaks were found, demonstrating the specificity of the analytical approach. The rat brain and plasma samples had linear standard plots in the range of "1–800 ng/mL" concentration with correlation coefficients of "0.9597" and

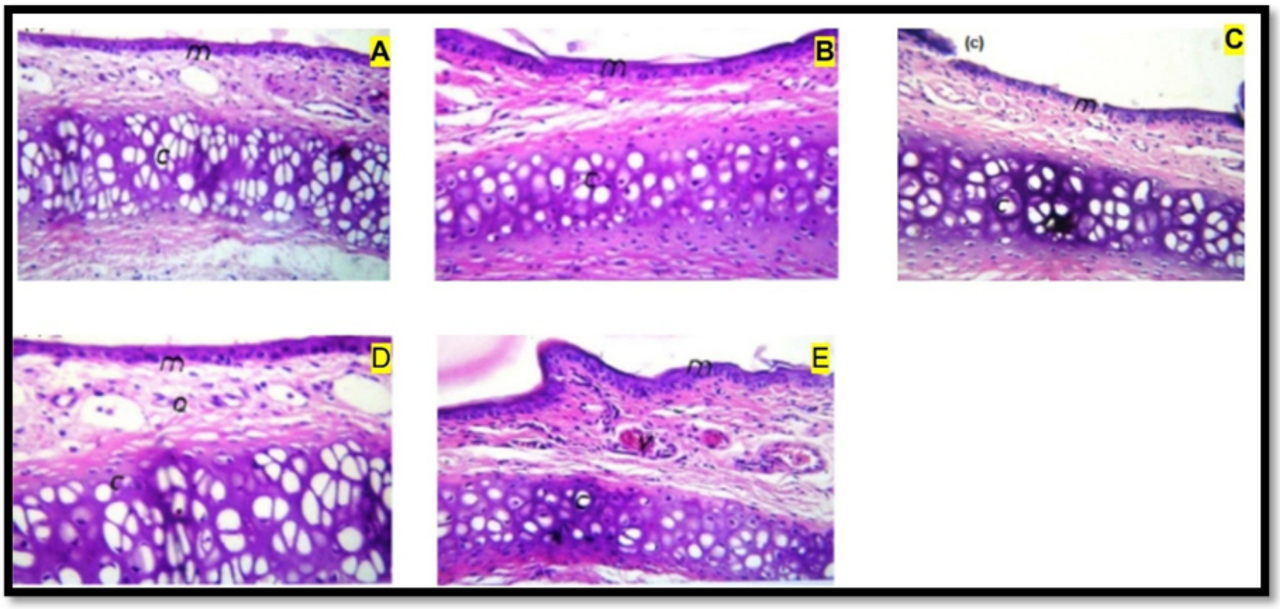

Figure 11 Light photomicrograph of (**A**) untreated rat epithelium and rat epithelium treated with (**B**) normal saline pH 6.8, (**C**) Drug solution, (**D**) F9 and (**E**) G2. "m", mucosa; "c", underlying cartilage; "o", lamina propria of the mucosal layer; "v", blood vessels in lamina propria.

"0.9894", respectively. The FVT-spiked percentage in the plasma sample ranged from 92.492 to 98.675, and the FVT-spiked percentage in the brain sample ranged from 88.694 to 97.358, ensuring consistency and effectiveness, as illustrated in Table 5.

Table 5 Pharmacokinetic Parameters, Brain Targeting Efficiency, and Direct Nose-to-Brain Transport Following Administration of FVT Formulations

Parameters	Tissue/Organ	Formulations of FVT		
		FVT Solution	F9	G2
C_{max}	Plasma Brain	43.29±13.59 16.46±06.45	670.51±24.36 118.34±14.29	452.87±35.67 495.84±1892
T_{max}	Plasma Brain	45.62 60.87	– 34	15 10
AUC_{0-360}	Plasma Brain	5737.16±184.53 1842.84±164.72	52,684.35±225.34 14,876.29±94.36	15,385.46±1231.26 36,484.28±1159.46
AUC ratio		0.32	0.2825	2.3713
F_a		11.96	100	29.47±0.26
F_r		100	-	268.79±0.59
$T_{1/2}$	Plasma Brain	152.36±12.35 228.43±5.64	98.37±8.34 133.84±9.03	15,857±11.56 198.37±8.64
MRT	Plasma Brain	226.07±15.69 331.86±29.64	116.87±6.59 184.35±5.38	162.63±10.29 273.84±7.64
DTE		121.84	-	874.18
DTP		18.23	-	89.42

Abbreviations: DTP, brain drug direct transport percentage; MRT, mean residence time; DTE, drug targeting efficiency; Fa absolute bioavailability; Fr, relative bioavailability.

Conclusion

The ratio of ethanol to PG is critical in decreasing the particle size of the FVT-loaded binary ethosome gel formula; meanwhile, low phospholipid concentration in binary ethosome was shown to have favorable entrapment efficiency. Carbopol showed better spreadability than HPMC in gel formulation. Based on enhancing the bioavailability and sustaining the drug release, it can be concluded that the Frovatriptan-Loaded Binary ethosome Gel as nano-delivery was developed as a promising non-invasive drug delivery system for treating migraine.

Disclosure

The authors report no conflicts of interest in this work.

References

1. Gupta S, Mehrotra S, Villalón CM, Perusquía M, Saxena PR, MaassenVanDenBrink A. Potential role of female sex hormones in the pathophysiology of migraine. *Pharmacol Ther*. 2007;113(2):321–340. doi:10.1016/j.pharmthera.2006.08.009
2. Aurora SK, Kori SH, Barrodale P, McDonald SA, Haseley D. Gastric stasis in migraine: more than just a paroxysmal abnormality during a migraine attack. *Headache*. 2006;46(1):57–63. doi:10.1111/j.1526-4610.2006.00311.x
3. Jassim Z, Jasim E. A review on strategies for improving nasal drug delivery systems. *Drug Invention Today*. 2018;10:2857–2864.
4. Hussein A, Jwad A, Majeed I, Mikhael E. The Effectiveness, Safety and Cost of Different Intranasal Steroid Sprays in Treating Iraqi Patients with Allergic Rhinitis: a Comparative Study. *J Pharm Biomed Sci*. 2015;5:61–66.
5. Ahmed Z, Sabri L, Al-Kinani K. Natural polymer Effect on gelation and rheology of ketotifen- loaded pH-sensitive in situ ocular gel (Carbapol). *J Adv Pharm Educ Res*. 2022;12:45–50. doi:10.51847/zOf4TcFeKT
6. Al-Wiswasi NN, Al-Khedairy EBH. Formulation and in vitro Evaluation of In-situ Gelling Liquid Suppositories for Naproxen. *Iraqi J Pharm Sci*. 2008;17(1):31–38. doi:10.31351/vol17iss1pp31-38
7. Mourad AM, Abdulla Z, Abbas MT, Fawzi HA. Role of Matrix Metalloproteinase–9 in the Pathogenesis of Preeclampsia. *Int J Women's Health Reprod Sci*. 2023;11(3):116–120. doi:10.15296/ijwhr.2023.20
8. Chhajed S, Sangale S, Barhate SD. ADVANTAGEOUS NASAL DRUG DELIVERY SYSTEM: a REVIEW. *Int J Pharm Sci Res*. 2011;2(6):1322–1336. doi:10.13040/IJPSR.0975-8232.2(6).1322-36
9. Silberstein SD, Shrewsbury SB, Hoekman J. Dihydroergotamine (DHE) - Then and Now: a Narrative Review. *Headache*. 2020;60(1):40–57. doi:10.1111/head.13700
10. Martin V, Hoekman J, Aurora SK, Shrewsbury SB. Nasal Delivery of Acute Medications for Migraine: the Upper Versus Lower Nasal Space. *J Clin Med*. 2021;10(11):2468. doi:10.3390/jcm10112468
11. Rapoport AM, Bigal ME, Tepper SJ, Sheftell FD. Intranasal medications for the treatment of migraine and cluster headache. *CNS Drugs*. 2004;18(10):671–685. doi:10.2165/00023210-200418100-00004
12. Younis YK, Alhammid SNABD. Intranasal Oleic acid-based nanoemulsion of Diazepam: design, formulation and in-vitro evaluation. *J Res Pharm*. 2023;27(2):529–543. doi:10.29228/jrp.335
13. Majeed IA. Comparative Evaluation of Using Intranasal Desmopressin, Parenteral Diclofenac or their Combination in the Management of Acute Renal Colic Pain in Iraqi Patients. *Iranian j Pharm Res*. 2007;16(2):1–4. doi:10.31351/vol16iss2pp1-4
14. Al-Tamimi JJI. Bioequivalence and Pharmacokinetics Comparison of Two Formulations of Extended-Release Pentoxifylline Tablets in Healthy Subjects after Fasting and Fed Conditions. *Iraqi J Pharm Sci*. 2015;24(2):60. doi:10.31351/vol24iss2pp53-60
15. Tepper SJ, Johnstone MR. Breath-powered sumatriptan dry nasal powder: an intranasal medication delivery system for acute treatment of migraine. *Medical Devices*. 2018;11:147–156. doi:10.2147/mder.s130900
16. Scott AK. Sumatriptan clinical pharmacokinetics. *Clin. Pharmacokinet.* 1994;27(5):337–344. doi:10.2165/00003088-199427050-00002
17. Buchan P, Keywood C, Wade A, Ward C. Clinical pharmacokinetics of frovatriptan. *Headache*. 2002;42 Suppl 2:S54–62. doi:10.1046/j.1526-4610.42.s2.3.x
18. Buchan P. The pharmacokinetics of frovatriptan (VML 251/SB 209509), a potent selective 5-HT1B/1D agonist, following single dose administration by oral and intravenous routes to healthy male and female volunteers. *Headache*. 1998;38(5):376.
19. Buchan P, Gay-Feutry C. In vitro metabolism of frovatriptan [poster]. *Eur J Neurol*. 2000;7(S3):81.
20. Jain AK, Khar RK, Ahmed FJ, Diwan PV. Effective insulin delivery using starch nanoparticles as a potential trans-nasal mucoadhesive carrier. *Eur J Pharm Biopharm*. 2008;69(2):426–435. doi:10.1016/j.ejpb.2007.12.001
21. Shen LN, Zhang YT, Wang Q, Xu L, Feng NP. Enhanced in vitro and in vivo skin deposition of apigenin delivered using ethosomes. *Int J Pharm*. 2014;460(1–2):280–288. doi:10.1016/j.ijpharm.2013.11.017
22. Nakhaei P, Margiana R, Bokov DO, et al. Liposomes: structure, Biomedical Applications, and Stability Parameters With Emphasis on Cholesterol. *Front Bioeng Biotechnol*. 2021;9:705886. doi:10.3389/fbioe.2021.705886
23. Younis YK, Alhammid ABD. Intranasal Oleic acid-based nanoemulsion of Diazepam: design, formulation and in-vitro evaluation. *J Res Pharm*. 2023;27(2):567.
24. Sherafudeen SP, Vasantha PV. Development and evaluation of in situ nasal gel formulations of loratadine. *Res Pharm Sci*. 2015;10(6):466–476.
25. Sulaiman HT, Jabir SA, Al-Kinani KK. Investigating the effect of different grades and concentrations of ph-sensitive polymer on preparation and characterization of lidocaine hydrochloride as in situ gel buccal spray. *Asian J Pharm Clin Res*. 2018;11(11):401–407.
26. Salih OS, Ghareeb MM. Formulation and In-vitro Evaluation of Thermosensitive Ciprofloxacin HCL In-situ Gel for Local Nasal Infection. *IJDDT*. 2021;11(4):57.
27. Yousif HS, Khalil YI. In situ gelling formulation of Naproxen for oral sustained delivery system. *Iraqi J Pharm Sci*. 2009;18(1):13–20.

28. Adnan M, Nief R, Abd-Al SN, Kharaba HA. Preparation and In-Vitro Evaluation of Floating Oral In-Situ Gel of Montelukast Sodium (Conference Paper). *Iraqi J Pharm Sci*. 2022;31(Suppl.):162–167. doi:10.31351/vol31issSuppl.pp162-167
29. Nief RA, Tamer MA, Abd Alhammid SN. Mucoadhesive oral in situ gel of itraconazole using pH-sensitive polymers: preparation, and in vitro characterization, release and rheology study. *Drug Invention Today*. 2019;11(6):1450–1455.
30. Alabdly A, Kassab HJ. Formulation Variables Effect on Gelation Temperature of Nefopam Hydrochloride intranasal in Situ Gel (Conference Paper). *Iraqi J Pharm Sci*. 2022;31(Suppl.):32–44. doi:10.31351/vol31issSuppl.pp32-44
31. Muslim RK, Maraie NK. Preparation and evaluation of nano-binary ethosomal dispersion for flufenamic acid. *Mater Today Proc*. 2022;57:354–361. doi:10.1016/j.matpr.2021.09.239
32. Jain S, Patel N, Madan P, Lin S. Quality by design approach for formulation, evaluation and statistical optimization of diclofenac-loaded ethosomes via transdermal route. *Pharm Dev Technol*. 2015;20(4):473–489. doi:10.3109/10837450.2014.882939
33. Lk E, Berkó S, Gácsi A, et al. Design and Optimization of Nanostructured Lipid Carrier Containing Dexamethasone for Ophthalmic Use. *Pharmaceutics*. 2019;11(12):679. doi:10.3390/pharmaceutics11120679
34. Abdulbaqi IM, Darwis Y, Khan NA, Assi RA, Khan AA. Ethosomal nanocarriers: the impact of constituents and formulation techniques on ethosomal properties, in vivo studies, and clinical trials. *Int j Nanomed*. 2016;11:2279–2304. doi:10.2147/ijn.S105016
35. Farzaneh H, Ebrahimi Nik M, Mashreghi M, Saberi Z, Jaafari MR, Teymouri M. A study on the role of cholesterol and phosphatidylcholine in various features of liposomal doxorubicin: from liposomal preparation to therapy. *Int J Pharm*. 2018;551(1–2):300–308. doi:10.1016/j.ijpharm.2018.09.047
36. Balakrishnan P, Park EK, Song CK, et al. Carbopol-incorporated thermoreversible gel for intranasal drug delivery. *Molecules*. 2015;20(3):4124–4135. doi:10.3390/molecules20034124
37. Zambaux MF, Bonneaux F, Gref R, et al. Influence of experimental parameters on the characteristics of poly(lactic acid) nanoparticles prepared by a double emulsion method. *J Control Release*. 1998;50(1–3):31–40. doi:10.1016/s0168-3659(97)00106-5
38. Pardeshi CV, Belgamwar VS. Direct nose to brain drug delivery via integrated nerve pathways bypassing the blood-brain barrier: an excellent platform for brain targeting. *Expert Opin Drug Deliv*. 2013;10(7):957–972. doi:10.1517/17425247.2013.790887
39. Garg AB, Aggarwal D, Garg SK, Singla AK. Spreading of semisolid formulations: an update. *Pharm Technol*. 2002;26:84–105.
40. Amarachinta PR, Sharma G, Samed N, Chettupalli AK, Alle M, Kim JC. Central composite design for the development of carvedilol-loaded transdermal ethosomal hydrogel for extended and enhanced anti-hypertensive effect. *J Nanobiotechnology*. 2021;19(1):100. doi:10.1186/s12951-021-00833-4
41. Chettupalli AK, Ananthula M, Amarachinta PR, Bakshi V, Yata VK. Design, Formulation, in-vitro and ex-vivo evaluation of atazanavir loaded cubosomal gel. *Biointerface Res Appl Chem*. 2021;11(4):12037–12054. doi:10.33263/BRIAC114.1203712054
42. Sallustio V, Farruggia G, Di Cagno MP, et al. Design and Characterization of an Ethosomal Gel Encapsulating Rosehip Extract. *Gels*. 2023;9(5):362.
43. Galgatte UC, Kumbhar AB, Chaudhari PD. Development of in situ gel for nasal delivery: design, optimization, in vitro and in vivo evaluation. *Drug Deliv*. 2014;21(1):62–73. doi:10.3109/10717544.2013.849778
44. Vipul V, Basu B. Formulation and characterization of novel floating in-situ gelling system for controlled delivery of ramipril. *Int J Drug Delivery*. 2013;5:43–55.
45. El-Shenawy AA, Mahmoud RA, Mahmoud EA, Mohamed MS. Intranasal In Situ Gel of Apixaban-Loaded Nanoethosomes: preparation, Optimization, and In Vivo Evaluation. *AAPS Pharm Sci Tech*. 2021;22(4):147. doi:10.1208/s12249-021-02020-y
46. Gaikwad V. Formulation and evaluation of In-Situ gel of metoprolol tartrate for nasal delivery. *J Pharm Res*. 2010;3(4):788–793.
47. Unnisa A, Chettupalli AK, Al Hagbani T, et al. Development of Dapagliflozin Solid Lipid Nanoparticles as a Novel Carrier for Oral Delivery: statistical Design, Optimization, In-Vitro and In-Vivo Characterization, and Evaluation. *Pharmaceuticals*. 2022;15(5):568. doi:10.3390/ph15050568
48. Prasad RR, Kumar JR, Vasudha B, Kumar CA. FORMULATION DEVELOPMENT AND EVALUATION OF ALLOPURINOL SOLID DISPERSIONS BY SOLVENT EVAPORATION TECHNIQUE. *Int J Appl Pharm*. 2018;10(4):168–171. doi:10.22159/ijap.2018v10i4.25311
49. Bakshi V, Amarachinta PR, Chettupalli AK. Design, Development and Optimization of Solid Lipid Nanoparticles of Rizatriptan for Intranasal delivery: invitro & Invivo assessment. *Mater Today Proc*. 2022;66:2342–2357. doi:10.1016/j.matpr.2022.06.329
50. Gowda D, Tanuja D, Mohammed SK, Desai JS. Formulation and evaluation of In-Situ gel of Diltiazem hydrochloride for nasal delivery. *Der Pharmacia Lettre*. 2011;3(1).
51. Underwood W, Anthony R. AVMA guidelines for the euthanasia of animals: 2020 edition. *Retrieved on March*. 2020;2013(30):2020–2021.
52. Alfi O, From I, Yakirevitch A, et al. Human Nasal Turbinate Tissues in Organ Culture as a Model for Human Cytomegalovirus Infection at the Mucosal Entry Site. *J Virol*. 2020;94(19):58. doi:10.1128/jvi.01258-20
53. Zheng J, Lin J, Ma Y, et al. Establishment of sheep nasal mucosa explant model and its application in antiviral research. *Front Microbiol*. 2023;14:1124936. doi:10.3389/fmicb.2023.1124936
54. Shelke S, Shahi S, Jalalpure S, Dhamecha D, Shengule S. Formulation and evaluation of thermoreversible mucoadhesive in situ gel for intranasal delivery of Naratriptan hydrochloride. *J Drug Delivery Sci Technol*. 2015;29. doi:10.1016/j.jddst.2015.08.003
55. Majithiya RJ, Ghosh PK, Umrethia ML, Murthy RS. Thermoreversible-mucoadhesive gel for nasal delivery of sumatriptan. *AAPS Pharm Sci Tech*. 2006;7(3):67. doi:10.1208/pt070367
56. Yaribeygi H, Hemmati MA, Nasimi F, et al. Sodium Glucose Cotransporter-2 Inhibitor Empagliflozin Increases Antioxidative Capacity and Improves Renal Function in Diabetic Rats. *J Clin Med*. 2023;12(11):3815.
57. Reagan-Shaw S, Nihal M, Ahmad N. Dose translation from animal to human studies revisited. *FASEB j*. 2008;22(3):659–661. doi:10.1096/fj.07-9574LSF
58. Zheng H, Xia Y, Qu S, et al. Pharmacokinetic Study of Frovatriptan Succinate Tablet After Single and Multiple Oral Doses in Chinese Healthy Subjects. *Drug Des Devel Ther*. 2021;15:2961–2968. doi:10.2147/dddt.S308958
59. Alshehri S, Hussain A, Altamimi MA, Ramzan M. In vitro, ex vivo, and in vivo studies of binary ethosomes for transdermal delivery of Acyclovir: a comparative assessment. *J Drug Delivery Sci Technol*. 2021;62:102390. doi:10.1016/j.jddst.2021.102390
60. Bshara H. Improvement of the bioavailability of buspirone HCl using intranasal delivery systems. *Al-Azhar J Pharm Sci*. 2012;45(1):86–102.

61. Meirinho S, Rodrigues M, Santos AO, Falcão A, Alves G. Intranasal Microemulsion as an Innovative and Promising Alternative to the Oral Route in Improving Stiripentol Brain Targeting. *Pharmaceutics*. 2023;15(6):1641.
62. Abo El-Enin HA, Mostafa RE, Ahmed MF, et al. Assessment of Nasal-Brain-Targeting Efficiency of New Developed Mucoadhesive Emulsomes Encapsulating an Anti-Migraine Drug for Effective Treatment of One of the Major Psychiatric Disorders Symptoms. *Pharmaceutics*. 2022;14 (2):410. doi:10.3390/pharmaceutics14020410
63. Faul F, Erdfelder E, Lang AG, Buchner A. G*Power 3: a flexible statistical power analysis program for the social, behavioral, and biomedical sciences. *Behavior Research Methods*. 2007;39(2):175–191. doi:10.3758/bf03193146
64. Charan J, Kantharia ND. How to calculate sample size in animal studies? *J Pharmacol Pharmacotherapeutics*. 2013;4(4):303–306. doi:10.4103/ 0976-500x.119726
65. Festing MFW. Design and Statistical Methods in Studies Using Animal Models of Development. *ILAR J*. 2006;47(1):5–14. doi:10.1093/ilar.47.1.5
66. Patra M, Salonen E, Terama E, et al. Under the influence of alcohol: the effect of ethanol and methanol on lipid bilayers. *Biophys J*. 2006;90 (4):1121–1135. doi:10.1529/biophysj.105.062364
67. Agrawal M, Tripathi DK. Recent advancements in liposomes targeting strategies to cross blood-brain barrier (BBB) for the treatment of Alzheimer's disease. *J Controlled Release*. 2017;260:61–77. doi:10.1016/j.jconrel.2017.05.019
68. Saha RN, Vasanthakumar S, Bende G, Snehalatha M. Nanoparticulate drug delivery systems for cancer chemotherapy. *Mol Membrane Biol*. 2010;27(7):215–231. doi:10.3109/09687688.2010.510804
69. Nakmode D, Bhavana V, Thakor P, et al. Fundamental Aspects of Lipid-Based Excipients in Lipid-Based Product Development. *Pharmaceutics*. 2022;14(4):831. doi:10.3390/pharmaceutics14040831
70. He J, Huang S, Sun X, et al. Carvacrol Loaded Solid Lipid Nanoparticles of Propylene Glycol Monopalmitate and Glyceryl Monostearate: preparation, Characterization, and Synergistic Antimicrobial Activity. *Nanomaterials*. 2019;9(8):1162.
71. Lee H-J. The Study of pH in Nasal Secretion in Normal and Chronic Rhinosinusitis. *J Rhinol*. 2009;16(2):105–109.
72. Rajendra KJ, Ramesh B, Velmurugan S. Development of a new single unit dosage form of propranolol HCl extended release non-effervescent floating matrix tablets: in vitro and in vivo evaluation. *J Appl Pharm Sci*. 2016;6(5):112–118.
73. Cho HJ, Ku WS, Termsarasab U, et al. Development of udenafil-loaded microemulsions for intranasal delivery: in vitro and in vivo evaluations. *Int J Pharm*. 2012;423(2):153–160. doi:10.1016/j.ijpharm.2011.12.028